Development of seismic fragility curves for mainshock-damaged reinforced-concrete structures

A. Réveillère, P. Gehl, D. Seyedi & H. Modaressi
Risks Division, BRGM,3 avenue Claude-Guillemin, BP36009, 45060 Orléans, France

SUMMARY:
This communication presents an original procedure to derive fragility curves for previously damaged structural systems. These damage state-dependent functions constitute an important component in the framework of time-dependent risk assessment. For instance, they are used to estimate the updated vulnerability of structures exposed to potential aftershocks, based on the knowledge of their damage state after the main seismic event. While the state-of-the-art method for deriving such functions relies on incremental dynamic analysis, the present work proposes an alternative approach based on (i) the application of sequences of ground-motion records to the undamaged structure in order to have a representative panel of structures in each damage state, and (ii) an innovative statistical treatment of the permanent residual drift of damaged structures $\Delta_{p,t0}$ to derive the fragility functions: the maximum transient additional drift ($\Delta_{\mathrm{t,max}} - \Delta_{p,t0}$) is correlated to the intensity measure of the ground motion, and the influence of the initial permanent drift is then eliminated by estimating its distribution for a given initial damage state. The developed procedure is applied to a single story reinforced-concrete frame with a concentrated plasticity model and fragility curves are proposed for various initial damage states.

Keywords: time-dependent vulnerability, damage accumulation, aftershock fragility, dynamic analyses

1. INTRODUCTION

Most of the seismic risk assessment tools only consider an initially undamaged structure hit by one mainshock event. However, structures may be initially damaged from past earthquakes, and a seismic sequence is commonly made of a mainshock followed by series of aftershocks. In this post-mainshock context, during which the structure is not repaired, the rate of earthquake occurrence is significantly increased (due to the presence of aftershocks) and the physical vulnerability of possibly mainshock-damaged buildings may also increase. In this context, the updated knowledge of the vulnerability of the damaged buildings is of critical importance to accurately assess the associated risk and guide building-occupancy policies after a main seismic event.

A methodology to derive fragility curves for structures which are initially in a given damage state is developed. Contrary to the widely used incremental dynamic analysis, successive dynamic analyses with a set of unscaled natural ground-motion records are performed. Several samples of structures in each damage state, which may differ by their local damage configuration, are generated. The current condition of the structure at a time t_0 is represented by its residual (or permanent) drift ratio $\Delta_{p,t0}$ at the end of the pre-t_0 events and the additional transient drift (i.e. the maximum transient drift minus the initial permanent one $\Delta_{\mathrm{t,max}} - \Delta_{p,t0}$) obtained from the next dynamic simulation is used to assess whether the structure will reach a higher damage state or not. The main part of the developed procedure is to find a probabilistic relation between the seismic intensity and this additional drift. Distribution of the permanent drift has to be estimated within each damage state for this purpose. Section 2 is devoted to the methodological developments and the description of the time-dependent risk assessment framework, which relies on the existence of state-dependent fragility curves. Finally, in section 3 the methodology is applied to a reinforced-concrete frame in order to derive state-dependent fragility curves.

2. METHODOLOGICAL DEVELOPMENTS FOR STATE-DEPENDENT FRAGILTIY CURVES

2.1. Time-dependent risk assessment framework

Previous studies (Luco et al., 2004, Yeo & Cornell, 2005; Ryu et al., 2011; Luco et al., 2011) have developed a methodology for time-dependent risk assessment. It relies on coupling the performance of the building at the risk-assessment time t_0 and the probabilistic hazard assessment during a considered time-span. The temporal position of the risk analysis is presented on Figure 2.1.

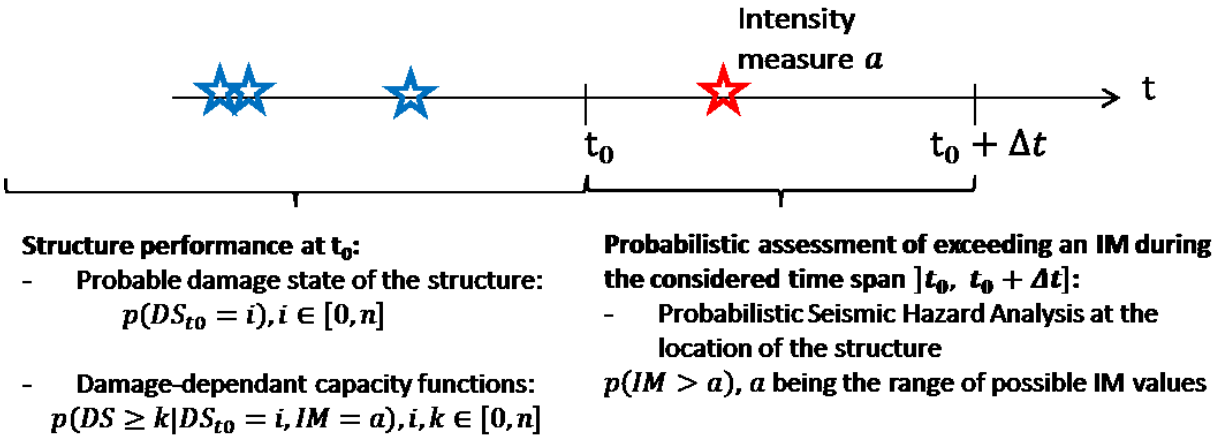

Figure 2.1. Schematic representation of the time-dependent risk assessment methodology at time t_0. It is based on the performance of the structure at that time t_0 and on the upcoming seismic risk during the time-span Δt.

The performance of the building at t_0 is by itself a combination of its current Damage State (DS) and of its capacity to withstand further seismic actions. The state of the building at t_0 is characterized by the probability of being in one of the n damage states (defined by an appropriate damage scale): $P(DS_{t0} = i);\ i \in [0, n]$.

For each of these possible initial damages states DS_{t0}, the capacity of the building needs to be estimated through state-dependent fragility curves, which give the probability for a structure in state DS_{t0} to reach or exceed a given damage state with respect to an Intensity Measure (IM) of a given level a: $P(DS \geq k | DS_{t0} = i, IM = a);\ k \in [1, n]$. Once these components are defined, the initial state of the structural system is described and its fragility to future earthquakes can be quantified as follows (Luco et al., 2011):

$$P(DS \geq k | IM = a) = \sum_{i=0}^{n} P(DS_{t0} = i) \cdot P(DS \geq k | DS_{t0} = i, IM = a) \quad (2.1)$$

In common practice, the building is considered to be initially intact ($DS_{t0} = 0$) and Equation 2.1 becomes trivial: $P(DS \geq k | IM = a) = P(DS \geq k | DS_{t0} = 0, IM = a)$. The more general formulation of Eq. 2.1 considering initially damaged structures enables to consider the time dependency and may be used in two main contexts:

- In the short term context, during post-mainshock emergency operations. Typically, in the literature, methodologies have been proposed to assess the safety of mainshock-damaged structures by coupling the aftershock hazard with the updated fragility. From this aftershock risk assessment, a building-occupancy policy is deduced (Yeo & Cornell, 2005). Similarly, by applying the same methodology to a bridge, Franchin et al. (2009) propose a traffic allowance policy.
- In the long term context, the time-span corresponds to the life-cycle of the building, which is exposed to damage accumulation as well (e.g. Yeo & Cornell, 2005).

After a mainshock, the assessment of the building state at time t_0 can be achieved through various techniques:

- Inspection-based or expert knowledge: it relies on post-seismic observations and the judgement of civil engineers on the actual damages of the inspected structures.
- Shakemaps (uncertain hazard): shortly after the occurrence of the seismic event, parameters such as magnitude and localisation are used to estimate shakemaps of the affected areas. Then, if a vulnerability study has been previously carried out, fragility curves can be used to estimate the damage probabilities of the buildings in the area.
- Instrumentation: seismic stations can record the seismic ground-motion around the affected area, thus giving a more accurate estimation of the hazard level. Also, for specific and critical structures, it is possible to perform building instrumentation in order to directly measure the lengineering demand on the structure.

As a result, there is a strong need to develop state-dependent fragility curves, which are a necessary step to perform risk assessment in the aftershock time-span. This issue is the subject of the next sub-sections.

2.2. Simulation strategy

Several past studies (Bazzuro et al., 2004; Ryu et al., 2011) propose to develop state-dependent curves using incremental dynamic analysis, i.e. a progressive scaling of the ground motion's amplitude without modifying their spectral shape (Vamvatsikos & Cornell, 2002) in order to have a sufficient number of buildings in each damage state. In this sub-section we present a methodology for developing DS-dependent fragility functions using a set of unscaled natural records. Ground-motions from this set are applied to the structure until each DS is populated with enough outcomes, which may have different local damage configurations. Damaged structures are then used to compute the response to the next ground shaking.

The Engineering Demand Parameter (EDP) used in this framework is $\Delta_{t,max}$ the maximum transient inter-storey drift ratio (ISDR), which can be linked to straightforward damage state thresholds (e.g. Rossetto & Elnashai, 2003). Moreover, the estimation of ISDR through dynamic simulations gives access to the residual permanent drift. We note this quantity $\Delta_{p,t0} = |\Delta_p(t_0)|$ since it is the value of the ISDR evaluated at the time t_0. In the time-dependent framework, the permanent drift is of paramount importance as it represents the updated initial conditions of the structure at t_0.

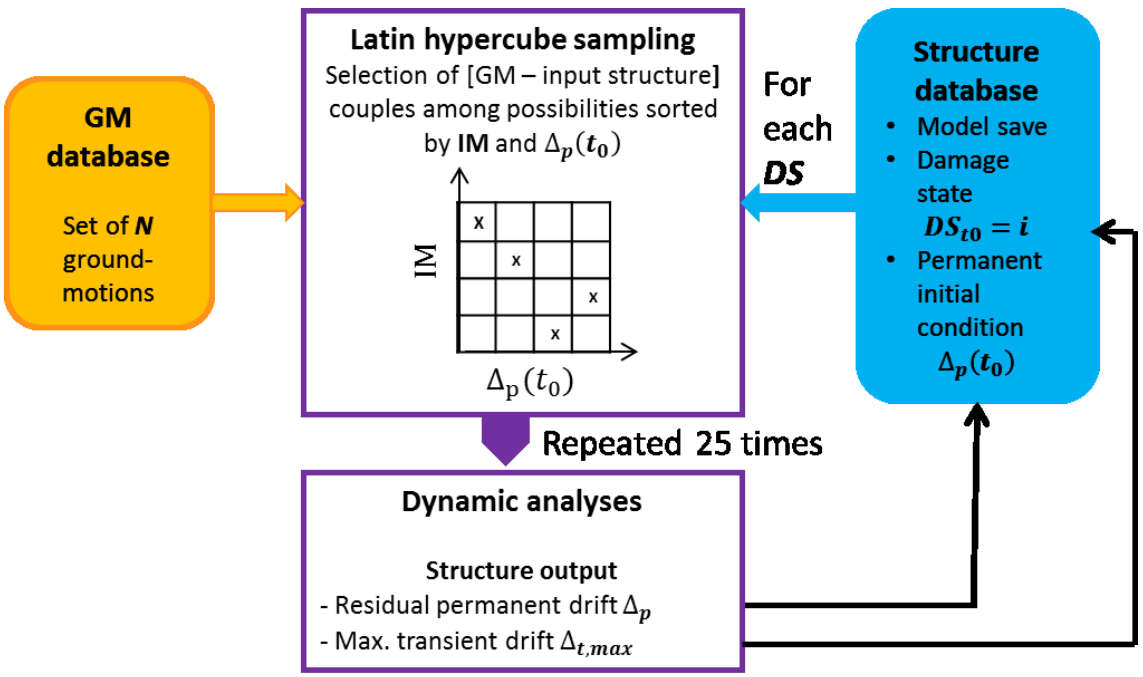

Figure 2.2. General simulation scheme for the dynamic analyses

The starting point of the study is a single structure in intact state, which we subject to a set of *N* time-histories. This first wave of analyses yields *N* new structures which are distributed along the different DS classes, depending on the recorded value of $\Delta_{t,max}$. For each initial damage state, 20 combinations of structures / ground-motion records are selected based on a Latin Hypercube Sampling procedure in order to test the range of possible combinations without introducing bias. This sampling methodology is applied to the structures of a DS class ranked based on their initial permanent drift $\Delta_{p,t0}$, and to the ground-motions ranked according to the intensity measure (IM) of interest (e.g. Sa or PGA). This step is repeated 25 times in order to populate each damage state with enough structures and to obtain a satisfying statistical significance (see Figure 2.2).

If some DS classes do not contain enough structures, it has been decided to reuse the damaged structures and recombine them until a sufficient number of outcomes in each DS class are reached. Thus, some of the results are obtained with structures that have been submitted to several time-histories. This remains a valid procedure in the sense that the chosen framework focuses on state-dependent curves and what occurred to the structure before t_0 have little influence on the future structural response. In the other word, what is important is the actual condition of the structural system at time t_0, which we choose here to be represented with the initial permanent drift $\Delta_{p,t0}$.

This approach enables to get a full representation of the possible outcomes in the different damage states. Therefore it has the advantage of accounting for the variability of the damaged structures when building DS-dependent fragility curves: different combinations of local damage mechanisms are translated into the residual permanent drifts, whose distribution is used to estimate the variability in initial conditions.

2.3. Modified regression technique for the estimation of damage distribution

Based on the recorded ISDR values, the objective is now to build the state-dependent fragility curves, defined as follows:

$$P(DS \geq k | DS_{t0} = i, IM = a) = \phi\left(\frac{\ln a - \ln \mu_{i,k}}{\beta_{i,k}}\right) \quad (2.2)$$

where ϕ is the cumulative distributive function of the standard normal distribution, and $\mu_{i,k}$ and $\beta_{i,k}$ are respectively the median and standard-deviation of the fragility curve from $DS=i$ to $DS \geq k$.
The regression technique (FEMA, 2000; Ellingwood & Kinali, 2009) is a widely used approach to derive fragility parameters (μ and β) for undamaged buildings. It relies on correlating the ISDR to the ground-motion IM: since the damage states can be identified by ISDR thresholds. A direct probabilistic relation between DS and IM is then deduced by a simple substitution of variables. In our specific case, we have to consider a structure with a permanent drift $\Delta_{p,t0}$ due to its loading history prior to t_0. We assume that the distribution of the maximum transient additional drift, $\Delta_{t,max} - \Delta_{p,t0}$, depends on the ground motion intensity a via the following relation:

$$\ln\left(\Delta_{t,max} - \Delta_{p,t0}\right) = \ln b + c \ln a + \varepsilon \quad (2.3)$$

The parameters b and c are obtained through the linear regression and ε is considered as a random variable with normal distribution of zero mean and standard deviation β_ε. Introducing drift thresholds, i.e. considering that the building reaches $DS \geq k$ when $\Delta_{t,max} \geq \Delta_{th,k}$, , the probability of reaching or exceeding damage state k for a building which has a permanent initial drift $\Delta_{p,t0} = \Delta_0$ is derived from equation (2.3) as follows:

$$P\left(DS \geq k \middle| \Delta_{p,t0} = \Delta_0, IM = a\right) = P\left(\varepsilon \leq \ln\left(\frac{b.a^c}{\Delta_{th,k} - \Delta_0}\right)\right) = \phi\left[\frac{\ln(b.a^c) - \ln\left(\Delta_{th,k} - \Delta_0\right)}{\beta_\varepsilon}\right] \quad (2.4)$$

For an initially damaged building ($DS_{t0}=i$), the permanent drift cannot exceed the threshold of the

higher damage state, $\Delta_{th,i+1}$, so we can assume that $\Delta_{p,t0}$ is in the range $[0; \Delta_{th,i+1}[$. If we note *f* the probability density function of the permanent drift, the DS-dependent probability can then be expressed as follows:

$$P(DS \geq k | DS_{t0} = i, IM = a) = \int_0^{\Delta_{th,i+1}} P\left(DS \geq k \middle| \Delta_{p,t0} = \Delta_0, IM = a\right) . f\left(\Delta_{p,t0} \middle| DS_{t0} = i\right) d\Delta_0 \quad (2.5)$$

The next step is to estimate *f*, the distribution of the permanent drift. The population of buildings that are initially in state $DS_{t0}=i$ corresponds to the buildings whose absolute ISDR is included between $\Delta_{th,i}$ and $\Delta_{th,i+1}$. Within this overall population we have to distinguish two sub-populations depending on the leaning side where that maximal ISDR has been reached (negative or positive values of permanent drifts). For each sub-population we assume a normal distribution of $\Delta_p(t_0)$, whose parameters are evaluated by fitting the permanent drifts from the simulation results. For simplifying the notations in this paper, we assume equal weights, equal standard deviation $\sigma_{\Delta_0,i}$ and opposite mean $\pm\mu_{\Delta_0,i}$ of these two sub-populations, which corresponds to symmetrical structure. A general formulation for non-symmetrical configurations would work identically. The probability density function of $\Delta_p(t_0)$ therefore reads as a combination of two normal distributions:

$$f\left(\Delta_p(t_0) \middle| DS_{t0} = i\right) = \frac{1}{2\sqrt{2\pi}\sigma_{\Delta_0,i}} \left[e^{-\frac{\left(\Delta_p(t_0) - \mu_{\Delta_0,i}\right)^2}{2\sigma^2_{\Delta_0,i}}} + e^{-\frac{\left(\Delta_p(t_0) + \mu_{\Delta_0,i}\right)^2}{2\sigma^2_{\Delta_0,i}}} \right] \text{ with } \Delta_p(t_0) \epsilon]-\Delta_{th,i+1}; \Delta_{th,i+1}[\quad (2.6)$$

Using the above equation, the distribution of $\Delta_{p,t0} = \left|\Delta_p(t_0)\right|$ can be deduced:

$$f\left(\Delta_{p,t0} \middle| DS_{t0} = i\right) = \frac{1}{\sqrt{2\pi}\sigma_{\Delta_0,i}} \left[e^{-\frac{\left(\Delta_{p,t0} - \mu_{\Delta_0,i}\right)^2}{2\sigma^2_{\Delta_0,i}}} + e^{-\frac{\left(\Delta_{p,t0} + \mu_{\Delta_0,i}\right)^2}{2\sigma^2_{\Delta_0,i}}} \right] \text{ with } \Delta_{p,t0} \epsilon [0; \Delta_{th,i+1}[\quad (2.7)$$

Finally, these distributions are used to compute the integral in Equation 2.5 and a lognormal cumulative distribution function is fitted to the curve in order to identify the DS-dependent fragility parameters $\mu_{i,k}$ and $\beta_{i,k}$ in Equation 2.2.

3. APPLICATION TO A SINGLE FRAME

3.1. Description of the structural model

To illustrate the developed methodology, we apply a set of ground-motion records to a single-story single-bay reinforced-concrete frame (3m high and 4m wide). The beams and columns behaviour is considered linear elastic and the damage mechanism is concentrated at the extremities, with the formation of plastic hinges (Zareian & Medina, 2010). The plastic hinges model developed by Ibarra & Krawinkler (2005) is used and its main parameters are presented in Table 3.1.

Table 3.1. Main parameters used in the plastic hinge model from Ibarra & Krawinkler (2005)

Parameter	**Column spring**	**Beam spring**
Elastic stiffness (kN.m)	70 000	150 000
Yield moment (kN.m)	52.5	210
Plastic Rotation capacity (rad)	0.015	0.02
Post-capping rotation capacity (rad)	0.161	0.133
Ultimate rotation capacity (rad)	0.4	0.4
Strain hardening ratio	0.0018	0.005
Residual strength ratio	0.2	0.2
Degradation parameter	1 000 (no degradation)	

The main parameters (e.g. yield and capping moment) used for this study correspond to beams and columns elements from a previous work (Seyedi et al., 2010) on a reinforced-concrete building. Values for undetermined parameters are adapted from the calibration presented by Haselton (2006). The elastic portion of the elements is assigned a Young modulus of 3.10^7 kPa, while the columns and beams have a respective section of 0.135m² and 0.197m².

We choose the Sa(T1) as the IM of interest for this structure, T1=0.195s being the period of the fundamental mode. The drift thresholds to identify the damage states are those proposed by Rossetto & Elnashai (2003) for the EMS-98 damage scale (D1 – Slight, D2 – Moderate, D3 – Heavy, D4 – Very heavy). The damage state D5 (Collapse) is not considered in this study, due to the difficulty to obtain reliable simulation results for collapse conditions.

3.2. Dynamic analyses

As explained in the previous section, the structure is submitted to successive ground-motions: in this case, we select a set of 175 time-histories from the European Ground-Motion Database (Ambraseys et al., 2004) that are indifferently used as mainshocks or aftershocks. The dynamic simulations are carried out using the OpenSees software. As an example, Figure 3.1 shows the behaviour of the frame submitted to a succession of time-histories (before and after t_0).

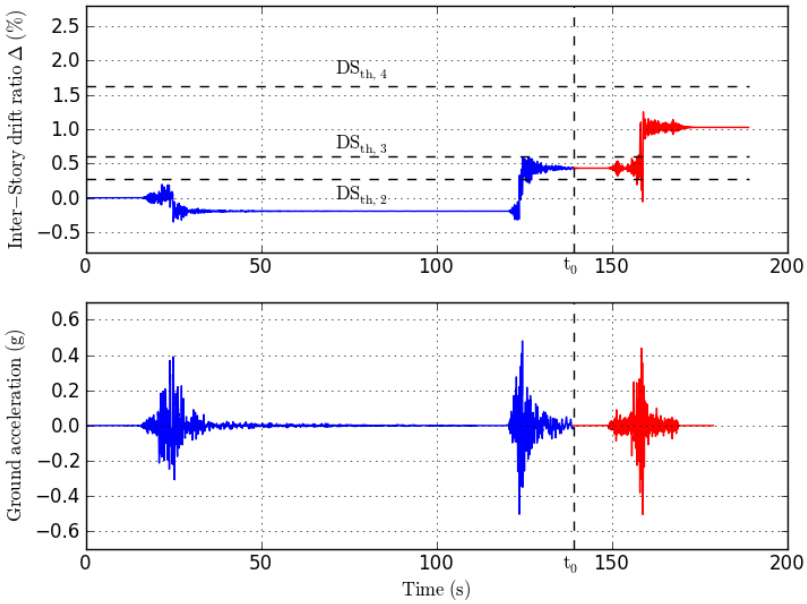

Figure 3.1. Example of successive time-history analysis; Prior to t_0, the structure has reached a damage state DS_{t0}=2 and has a permanent drift $\Delta_{p,t0}$. After t_0, the ground-motion of IM=a (red part, bottom panel) brings the structure to DS=3. The correlation is estimated between $(\Delta_{t,max} - \Delta_{p,t0})$ and a.

The results of the repeated dynamics analyses are used to perform the regression between the intensity measure and the additional drift, and also to identify the distribution of the permanent drift within each damage state for computing $f(\Delta_{p,t0})$. Figure 3.2 illustrates the methodology for the structures with an initial damage state DS_{t0}=2. The top histogram shows the actual distribution of the initial permanent drifts. The right histogram represents the set of ground-motions considered for the simulation. The central panel shows the combination of these parameters that have been chosen for performing the simulations, and the colours on the points indicate the results: yellow if the structure has remained in DS_{t0}=2, resp. red and black if it has increased to resp. DS=3 or 4.

On the top histogram of Figure 3.2, we can clearly see the bimodal normal distribution of the permanent drift (a mixture of two Gaussian distributions): using the Expectation Maximization algorithm, the two sub-populations can be distinguished (i.e. buildings that have reached the DS threshold on the positive or negative direction) and the parameters of $f(\Delta_{p,t0})$ are finally estimated.

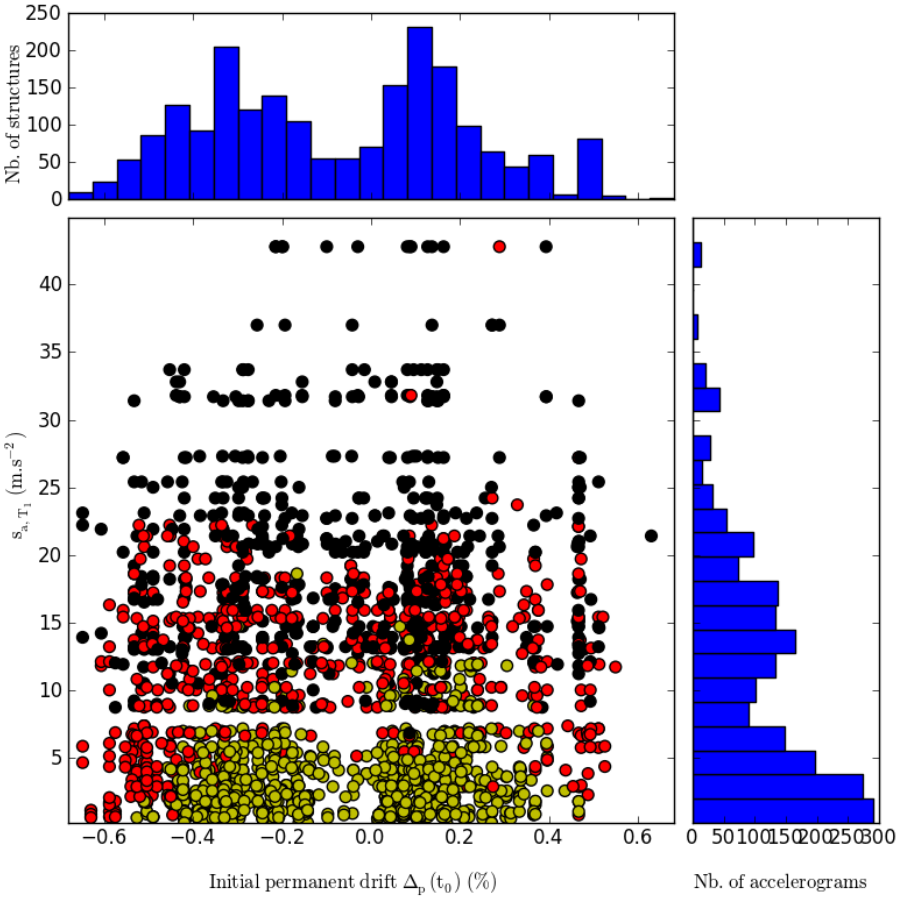

Figure 3.2. Damage states obtained (coloured dots, yellow, red and black corresponding resp. to DS=2, 3 and 4) depending on the IM Sa(T1) of the aftershock and on the initial permanent drift $\Delta_p(t_0)$ of the structures. The top histogram shows the repartition of permanent drifts for the initial damage state $DS_{t0} = 2$

The simulation results are finally used to perform a linear regression between $\ln Sa(T1)$ and the quantity $\ln(\Delta_{t,max} - \Delta_{p,t0})$. As an example, this regression is plotted in Figure 3.3. Blue points represent the relation for all previously damaged structures (with $\Delta_{p,t0} > 0$) and the red ones are the regression for only initially intact structures (with $\Delta_{p,t0} = 0$). For both cases the slope of the linear fit is almost the same.

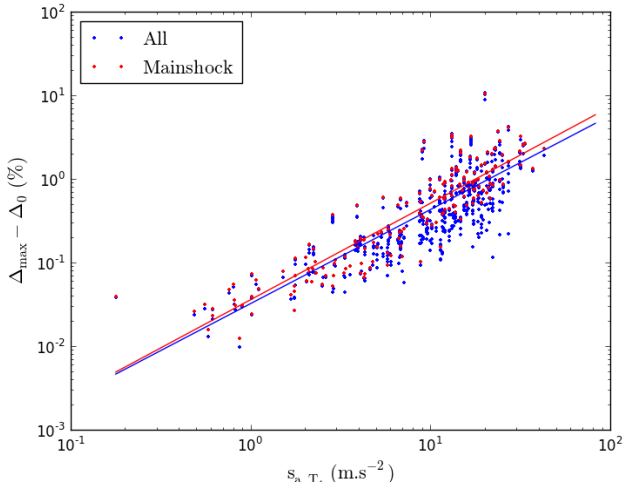

Figure 3.3. Comparison of the regression results for the undamaged buildings (in red) and the initially damaged ones (in blue)

The fact that all buildings, whatever their initial conditions, experience a similar dynamic response is due to the choice of the model for the plastic hinges: no cyclic degradation has been taken into account, therefore the model continues to display the same stiffness and the only evolution is the deformations in the hinges, which are progressively moving towards the next drift threshold. Consequently, in this specific case, the only influent parameter is the value of the permanent drift, indicating how close the building is to the next drift threshold. Following this logic, it can finally be argued that only mainshock simulations are needed and the damaged structures can be artificially modelled by adding a permanent drift or decreasing the drift threshold.

3.3. Derivation of state-dependent fragility curves

The results of the application of the modified regression technique (see sub-section 2.3) to the non-linear dynamic analyses are presented in Table 3.2. The results consist in the $\mu_{i,k}$ and $\beta_{i,k}$ parameters defined in Equation 2.2 for describing the transition probabilities from DS_{t0}=i to DS=k.

Table 3.2. Parameters describing the transition probabilities from DS_{t0}=i to DS=k

initial DS (i)	DS_{t0}=0 (intact)		DS_{t0}=1		DS_{t0}=2		DS_{t0}=3	
future DS (k)	$\mu_{0,k}$	$\beta_{0,k}$	$\mu_{1,k}$	$\beta_{1,k}$	$\mu_{2,k}$	$\beta_{2,k}$	$\mu_{3,k}$	$\beta_{3,k}$
1	3.51	0.58	-	-	-	-	-	-
2	6.65	0.58	5.18	0.70	-	-	-	-
3	12.58	0.58	11.30	0.66	8.94	0.74	-	-
4	32.75	0.58	31.64	0.66	29.76	0.66	22.05	0.71

The median parameters in Table 3.2 show, as expected, the capacity reduction of the frame, as previously damaged structures tend to have higher probabilities (i.e. lower median values of IM) of reaching further damage states due to an aftershock. It can also be noted that the standard deviation is higher for initially damaged structures: this is explained by the distribution of initial permanent drift, which is the source of additional uncertainties, as opposed to the initial undamaged structure, which state is well defined. Using the estimated fragility parameters, the DS-dependent fragility curves are plotted and displayed in Figure 3.4. Increasing initial damage resulting from past shocks (from solid black to light grey) is responsible for the translation of the fragility curves from the right to the left.

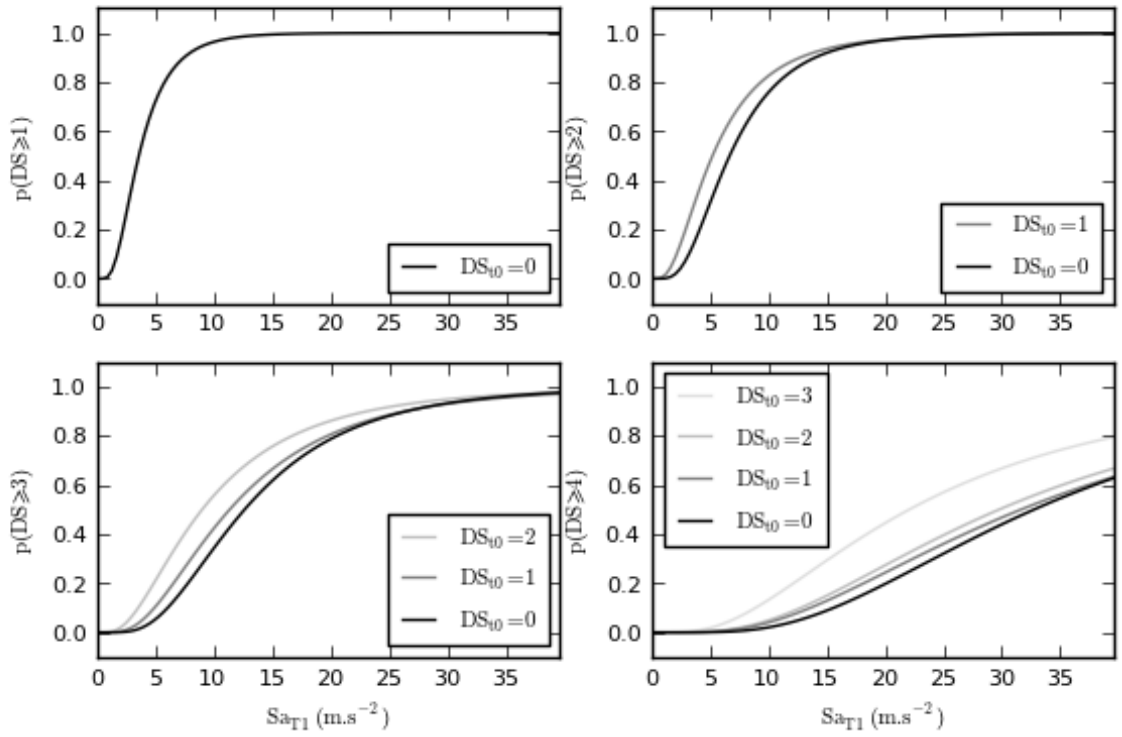

Figure 3.4. State-dependent fragility curves using the parameters in Table 3.2

4. CONCLUSION

In this study, we have proposed an original approach to derive fragility curves for previously damaged structural systems. These fragility functions give the transition probability for one damage state to another and they may therefore be referred as state-dependent fragility curves. The procedure presented here relies on the application of successive sets of unscaled ground-motion records. The key concept is the permanent drift ratio that is used to represent the starting conditions of initially damaged structures. This approach has been applied to a single reinforced-concrete frame and the resulting fragility curves show as expected the higher vulnerability of structures that have been previously damaged. Another important lesson from the application is that the chosen model for the plastic hinges does not induce any important change in the dynamic behaviour of the structure after successive time-histories: a very similar relation (i.e. slope of the regression) between the IM and EDP is found whether the structure is initially intact or damaged. This observation confirms that in this particular case (single-degree-of-freedom structure without cyclic degradation) the only important parameter is how "far" a structure with an initial permanent drift is from the higher drift threshold. Therefore future work could include the application of the procedure to more elaborate cases such as multi-degree-of-freedom structures with cyclic degradation. Finally, instead of the drift ratio, the use of EDPs that account for cyclic damages, like the Park & Ang (1985) index, could also be relevant in the specific case of state-dependent fragility curves.

AKCNOWLEDGEMENT

The research leading to these results has been carried out in the frame of the MATRIX Project, funded by the European Commission's Seventh Framework Program [FP7/2007-2013] under grant agreement n° 265138.

REFERENCES

Ambraseys, N.N., Douglas, J., Sigbjörnsson, R., Berge-Thierry, C., Suhadolc, P., Costa, G. and Smit, P.M. (2004). Dissemination of European Strong-Motion Data, vol. 2 using Strong-Motion Datascape Navigator. CD-ROM collection, Engineering and Physical Sciences Research Council, U.K.

Bazzurro, P., Cornell, C.A., Menun, C.A. and Motahari, M. (2004). Guidelines for seismic assessment of damaged buildings. *Thirteenth World Conference on Earthquake Engineering*, Vancouver, B.C., Canada.

Ellingwood, B.R. and Kinali, K. (2009). Quantifying and communicating uncertainty in seismic risk assessment. *Structural Safety* **31:2**.

FEMA (2000). Recommended seismic design creteria for new steel moment frame resisting buildings. Report no. FEMA-350, SAC Joint Venture, Washington D.C.

Franchin, P. and Pinto, P.E. (2009). Allowing traffic over mainshock-damaged bridges. *Journal of Earthquake Engineering* **13**, 585–599.

Haselton, C.B. (2006). Assessing Seismic Collapse Safety of Modern Reinforced Concrete Moment Frame Buildings, Ph.D. Dissertation, Department of Civil and Environmental Engineering, Stanford University Stanford, CA.

Ibarra, L.F. and Krawinkler, H. (2005). Global collapse of frame structures under seismic excitations. Technical Report 152, The John A. Blume Earthquake Engineering Research Center, Department of Civil Engineering, Stanford University, Stanford, CA.

Luco, N., Bazzurro, P. and Cornell, C.A. (2004). Dynamic versus static computation of the residual capacity of a mainshock damaged building to withstand an aftershock. *Thirteenth World Conference on Earthquake Engineering*, Vancouver, B.C., Canada.

Luco, N., Gerstenberger, M.C., Uma, S.R., Ryu, H., Liel, A.B. and Raghunandan, M. (2011). A methodology for post-mainshock probabilistic assessment of building collapse risk. Ninth Pacific Conference on Earthquake Engineering, Auckland, New Zealand.

Park, Y. and Ang, A. (1985). Mechanistic Seismic Damage Model for Reinforced Concrete. *Journal of Structural Engineering* **111**, 722-739.

Rossetto, T. and Elnashai, A. (2003). Derivation of vulnerability functions for European-type RC structures based on observational data. *Engineering Structures* **25**, 1241–1263.

Ryu,H., Luco, N., Uma, S.R. and Liel, A.B. (2011). Developing fragilities for mainshock-damaged structures through incremental dynamic analysis. Ninth Pacific Conference on Earthquake Engineering, Auckland, New Zealand.

Seyedi, D.M., Gehl, P., Douglas, J., Davenne, L., Mezher, N. and Ghavamian, S. (2010) Development of seismic fragility surfaces for reinforced concrete buildings by means of nonlinear time-history analysis. Earthquake *Engineering and Structural Dynamics* **39:1**,91–108.

Vamvatsikos, D. and Cornell C.A. (2002). Incremental dynamic analysis. *Earthquale Engineering and Structural Dynamics* **31:3**, 491-514.

Yeo, G.L. and Cornell, C.A. (2005). Stochastic characterization and decision bases under time-dependent aftershock risk in performance-based earthquake engineering. PEER Report 2005/13, Department of Civil and Environmental Engineering, Stanford University, Stanford, CA.

Zareian, F. and Medina, R.A. (2010). A practical method for proper modeling of structural damping in inelastic plane structural systems. *Computers & Structures* **88:1-2**, 45-53.